Linear Thermal Power Controller Design and Implementation for Efficient Electric Heating*

Jairo Nevarez, H. Bora Karayaka, Martin L. Tanaka and Peter Tay

School of Engineering and Technology
Western Carolina University
Cullowhee, North Carolina 28723, USA

***Abstract* - A prototype enclosure that is built for space heating was equipped with a resistive heater element and two temperature sensors. During a one-hour temperature regulation experiment, a Bang-Bang controller like those commonly used for residential heating control was used and the results were compared to a novel linear controller developed for the same purpose. The variables of comparison include temperatures and electrical power data. The study focuses on the linearization of the control system using a power electronics converter. The input of the converter must have linear relationship with the output power provided to the thermal system. Linearization was achieved by identifying a mathematical relationship that eliminates quadratic power function as well as converter's nonlinearity. This relationship was further implemented in the microcontroller. A second order linear mathematical model was later developed to identify and estimate the thermal circuit parameters utilizing a one-hour test facilitated through this new controller. Comparative results between simulation and experimental work validated the linearity of power control. Temperature disparity and input power characteristics were also improved using this new converter for controlling the space heater. The system developed is an important step toward energy savings, temperature improvements and demand side management for reducing peak demand.**

***Index Terms* – Linearizing, Closed Loop Controller, Thermal System, Buck Converter**

NOMENCLATURE

m	Slope of linear proportion
D	*Duty Cycle*
L	Inductor Value
R	Resistor Value
f_s	Switching frequency
P	Power to the thermal system
V	Voltage across the thermal load
V_{in}	Input Voltage to Buck Converter
I_{Lcrit}	Critical current of Inductor
$T_c(s)$	Controller transfer function
d_R	Output of the controller
$k_e()$	Linearization function comprising PWM
d_A	Output of k_e
BC	Buck Converter
e	Error signal
$k(s)$	Transfer function of linearized actuator
$T_{TH}(s)$	Transfer function of the thermal system
$T_C(s)$	Transfer function of the controller
T_{out}	Temperature output of the system
T_{ref}	Reference temperature
$T_{measured}$	Measured temperature of the system
K_p	Gain of Proportional Controller

*This work is supported by the Graduate School and Research at Western Carolina University.

I. INTRODUCTION

Ideally the load demand for a power system should be constant, which can be met by constant generation as well. Since this is not possible, utility companies must forecast and schedule generation for power demand. This causes power production during hours with peak demand to be expensive. Utility companies to keep up with peak load demands must adjust by producing more energy utilizing peak load power plants such as hydro and gas plants, which generally adds to the cost to produce power. Utility companies may also opt to purchase power from other utilities within the same continental interconnection, which also adds to the cost of power production. Most energy consumption of US single-family residential homes is from controllable appliances [1]. It would be beneficial (cost saving) if peak power demand was decreased in single-family residential homes.

This paper focuses on reducing the peak power for Thermostatically Controlled Loads (TCL). There are two major methods for reducing the peak power for TCL such as electric water heaters, air conditioners, refrigerators, heat pumps, etc. The classical Demand Side Management (DSM) method is demand (load) shifting or by utilizing energy efficient appliances. The demand shifting method requests households to utilize appliance during non-peak hours or by imposing pricing tariffs during peak hours. The main goal of this study is to minimize the cost of energy consumption for existing space heating appliances by improving energy efficiency and reducing peak power demand. A typical controllable space heating appliance utilizes a simple two-state Bang-Bang feedback controller. This paper describes a thermostatically controlled space heater using a Buck Converter (BC) as a linear power actuator. A simulation based on the mathematical model of the proposed system is used to determine the performance of the proposed linear thermal power controller. The simulation of the space heater's thermal circuit is based on a transfer function that is a second order mathematical model, which had been experimentally identified in [2]. The proposed linear control method is compared against the traditional Bang-Bang

controller for saving energy and improving temperature disparity.

This paper is organized as follows: Section II identifies related work in literature. Section III presents the proposed linear BC control system. The simulation and actual implementation of the proposed system is provided in Section IV. The experimentation and results that validate the robustness of the linear BC power controller's energy efficiency and reduced temperature variance over the typical Bang-Bang controller are presented in Section V. Finally, conclusions and future works are presented in Section VI.

II. Relevant Work

This section focuses on the demand side management methods for TCL. The first work concentrates on a direct-load algorithm of electric water heaters. The second review item investigates temperature control through K-factor control approach. The work in this paper is a continuation of the future work proposed in [2]. Although only the work in [2] and [3] are present in this section, other related studies can be found in reference [4] and [5].

A. Water Heater Load Potential

In [3] the direct-load control algorithm is presented to control a two-element electric water heater (EWH) for the purpose of load regulation. Major operational problems in power systems have been identified as an increased ramp rate and capacity requirements. Some options that could provide fast-response ancillary services include pumped-hydro plants, flywheels, batteries, DSM, and distributed generation resources. DSM is the option that has been the least explored and utilized. Due to strict telemetry requirements, most of the participants have been industrial consumers. However, a smart grid can provide more flexible tools to residential and commercial customers as highlighted in [3].

There are two control methods for DSM, direct and indirect load control. Direct load control is done through the utility company and gives little control to the consumer. This is very efficient but does not consider personal preferences. Indirect load control is set by the consumer or by appliances where peak hour usage is not allowed. For a Thermostatically Controlled Appliance (TCA) to be suitable for regulation it must always be in operation in order to be continuously monitored. That is the reason [3] concentrates on the direct control of EWH.

A conventional EWH in the United States has two heating elements. Only one element can be turned on at a time. The water in the tank is divided into hot water on the top, cold water on the bottom due to the thicker density, and a mixing layer in the middle. A thermostat is located in the hot water level and the cold-water level.

A modified circuit was used to control only the bottom heating element. The circuit checked the temperature of the water every minute. Changes to the element were limited to five minutes so that there was not a constant off-on action. The average load of the EWH is a continuously changing curve, though the power load is an irregular pulse train. The modified circuit is shown in Fig 1.

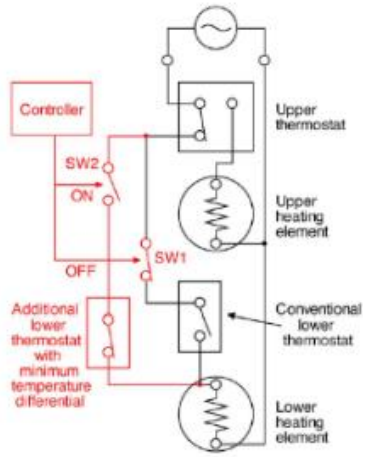

Fig. 1. EWH modified circuit

The results of this study indicate that DSM with a smart grid is possible and could be monetarily rewarding for customers. The simulations showed that multiple EWHs using a direct-load control could provide a 2-MW regulation service, also accounting for a customer with regular water consumption. The modeling results concluded that continuous 2-MW regulation service for 24-hour would take approximately 33,000 EWHs, but the load regulation service between 6:00 a.m. to midnight, only requires 20,000 EWHs.

B. Thermal Load Characterization and Regulation

As noted in [2], there are two main types of power plants, base load plants and peak load power plants. Base load plants are made to generate continuous reliable power at low cost. Examples of base load plants are coal, solar, and wind power plants. Peak load power plants have a fast ramp rate and are utilized during peak load hours.

Examples of peak load power plants are hydro and gas fired power plants. There are two primary methods that utility companies use to reduce peak power times. Peak power times are times in which electricity is in highest demand and as a result the most expensive. Increasing production during peak power times generally increases the cost to produce electricity. Utility companies typically attempts to reduce peak power demand by pricing tariffs and/or encourage customers to shift when they use electricity during peak hours. The second method that could be used is direct load control. For example, changing the temperature set-point of consumer appliances directly by the power company.

For single family, residential homes, much of the energy consumption comes from controllable appliances. Some examples of controlled appliances include electric water heaters, ovens, air conditioning, refrigerators, and dish washers. One significant method to promote more leveled power demand is to draw power continuously rather than drawing power in pulses. The proposed strategy in [2] replaced traditional Bang-Bang controller with the PI controller designed through K-factor approach on a thermal system model that was identified as shown in Fig 2. The actuator in this system was also a buck converter that regulated power to the load continuously, though in a non-linear fashion.

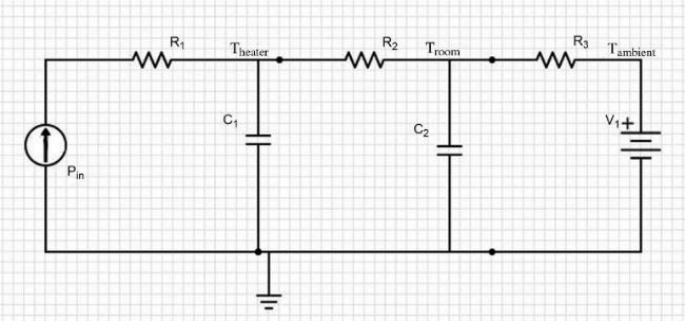

Fig. 2. Thermal system model.

For the conclusion, work in [2] claims that the methodology had five benefits over Bang-Bang controllers. The benefits were reduced peak power, smoothened ramp rates, eliminated in rush currents, constant power, and improved temperature stability. The conclusion in [2] suggested future research to improve energy efficiency of TCLs.

III. The Proposed BC Power Control System

Fig. 3 is a block diagram of the proposed control system in *s* domain. The feedback system consists of a proportional controller, signal conditioning system to linearize the BC, BC, the thermal system, and a temperature sensor. The input to the proposed feedback system is a setpoint temperature and the actual ambient temperature.

A. Proportional Controller

A proportional controller is a linear controller in which the output is calculated by multiplying the error with a constant. The constant is known as the proportional gain K_p and is varied by how the system needs to react. Because the controller system is a proportion of the error this often causes steady-state error.

$$d_R(t) = K_p \times e(t) \tag{1}$$

The error of the feedback system $e(t)$ is calculated simply by subtracting the reference or set point temperature and the measured temperature of the system.

$$e(t) = T_{ref} - T_{measured} \tag{2}$$

B. Linearizing the BC Power Actuator

The BC takes a pulse width modulated (PWM) input signal d_A and produces an output voltage or power P. The BC used in the experimentation can operate at a wide range of switching frequencies. However higher frequencies were prone to higher

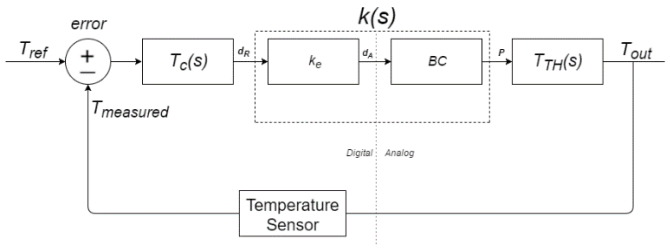

Fig. 3. Control system block diagram

distortion. The BC output voltage is determined by the duty cycle of the PWM. This relationship is linear [2]. However, the BC input duty cycle vs. output power relationship is not linear. This is because of the fact that the power produced for a resistive thermal load is proportional to the squared value of voltage applied to the heater. This study aims for a linear relationship between the input d_R (duty cycle), which determines the BC PWM duty cycle and output heater power. That is

$$P = c \times d_R \tag{3}$$

where c is a constant and P is output power of the BC.

Another important concern that impacts the linearity for a BC is discontinuous conduction mode (DCM). If the BC enters DCM the voltage to PWM duty cycle ratio would no longer be linear. The critical inductor current for the system can be found:

$$I_{Lcrit} = \frac{V_{in}}{2Lfs} D(1 - D) \tag{4}$$

where V_{in} is supply voltage of the BC, L is the BC inductor, fs is BC swicthing frequency, D is BC PWM duty cycle, and I_{Lcrit} is the BC critical inductor current. When the current through the BC inductor falls below I_{Lcrit} then the input and output of the BC is no longer linear.

The power used by the thermal system can be found using Ohm's law for power:

$$P = \frac{{V_{out}}^2}{R} \tag{5}$$

where V_{out} output voltage of BC, R heater load resistance, and P is power.

A problem with this power formula of equation (5) as mentioned earlier is that it does not represent a linear relationship between BC voltage and power. Therefore, a linear relationship between the power and duty cycle relationship of the system needs to be established by introducing a *k(s)* tranfer function.

$$k(s) = c \tag{6}$$

Empirical evidence has shown that the BC voltage and d_A relation can be approximated by (7). Fig. 4 shows the linear relationship between V_{out} and d_A determined through linear regression analysis.

$$V_{out} = 79.7 d_A + 8.34 \tag{7}$$

In order to obtain (6) or (3), d_A can be solved from (5) and (7) as follows

$$d_A = \frac{\sqrt{d_R \times c \times R} - 8.34}{79.7} \tag{8}$$

Nonlinear relationship given by (8) practically defines k_e block shown in Fig. 3. The k_e function can therefore be represented as:

$$d_A = k_e(d_R) \tag{9}$$

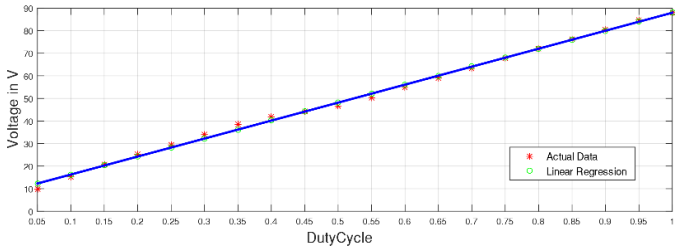

Fig. 4. BC voltage V_{out} and d_A comparison of the proposed control system.

Although k_e is a nonlinear function, it would result in a linear transfer function $k(s) = c$ when combined with the BC. Experimental analysis showed that the BC goes into DCM as dictated by (1) below 5 % duty cycle. As a result the voltage to duty cycle ratio is no longer linear. Thus k_e block output was limited as such from 0.05 to 1.0.

Since d_R is a product of the error and the proportional controller gain, the error needs to be limited to only positive values. Otherwise, negative error would result in a complex d_R as can be seen in (8).

The constant c is selected as 88 to compensate for the full range of 0.05 to 1.0 for k_e. If c was not set appropriately, the BC would not be able to utilize the full range and the system would suffer in performance. The load resistance R is empirically determined as 84Ω. This value reflects the multimeter value of the resistive heater load of the system.

C. *Temperature Averaging*

Due to the noise in the real time data acquisition medium caused by various means such as electromagnetic interference and analog digital conversion, there is a need to compensate for outliers in temperature sensing. Temperature sampling in this study occurs every 500 ms. For every sampling, an array is built by multiple back to back temperature readings. The elements in these array are later averaged using (10). These readings are compared against one another since temperature cannot change very fast between these readings. If the absolute error was greater than the allotted tolerance, the array element was set to 0, therefore not included in averaging. If all elements of the array are set to zero, the average temperature is set to the old temperature sample in memory.

$$\bar{x} = \frac{1}{n}\sum_{i=0}^{n-1} x_i = \frac{1}{n}(x_0 + \ldots + x_{n-1}) \tag{10}$$

D. *Infinite Impulse Response (IIR) Filter*

An IIR filter is also utilized to condition and smooth the data. The filter is applied to the system twice, for the acquisition of temperature and the output of k_e to succor the performance of the BC. The transfer function of the first order IIR filter is constructed as follows

$$H(z) = \frac{Y(z)}{X(z)} = \frac{m}{1-(1-m)\,z^{-1}} \tag{11}$$

where $X(z)$ and $Y(z)$ are the z-transforms of the input signal and output signal respectively. In addition

$$m = \frac{T_s}{\tau + T_s} \tag{12}$$

where T_s (sampling time) is 0.5 s, and τ (filter time constant) is 1.5 s. Since $\tau \geq 2T_s$, Nyquist/Shannon sampling theorem guarantees no aliasing occurs.

Based on the values of τ and T_s, m can be calculated as follows:

$$m = \frac{0.5}{1.5+0.5} = 0.25 \tag{13}$$

Resulting discrete time filter equation can be written accordingly as,

$$y(n) = 0.25x(n) + 0.75y(n-1) \tag{14}$$

The filter is designed to mostly consider the previous value of the data iteration, this could be adjusted accordingly by adjusting the time constant of the filter.

IV. Materials and Methods

An mbed LPC1768 microcontroller board based on Advanced RISC Machines (ARM) core was used to control the duty cycle of an amplified pulse-width modulated signal. This signal switches a high speed metaloxide semiconductor field-effect transistor (MOSFET). Switching of the MOSFET governs the DC output of a buck-boost converter voltage. The BC schematic is shown in Fig 5. The voltage of the resistive heating element is ultimately controlled by the manipulation of the duty cycle in PWM signal generated by the ARM microcontroller.

An open-loop control system is a control system in which the control (regulating) action is independent of the output [6]. In addition, open-loop systems have no automatic correction to the output of the system [7]. Therefore, measuring the open loop system output voltage with no outside influence gives a base output voltage to duty cycle relation. Thus, voltage measurements to the resistive heating load by modifying the duty cycle were first documented. The empirical tested values of single-input, single output system (SISO) system shows the input to output ratio i.e. the voltage to duty cycle relation could be represented by a line as shown in Fig. 4.

The next part of the research consists of some closed loop system techniques. A feedback-loop system is a process where the output of the system is continuously monitored and compared with the reference or set point [8]. The set point represents the desired value and, in this case, the reference is a constant value representing a desired temperature of a heated space or enclosure (Fig. 6).

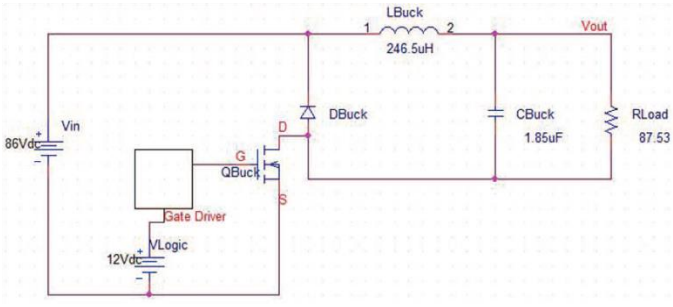

Fig. 5. Buck converter schematic [2].

Fig. 6. Temperature controlled enclosure and experimental setup

The heated enclosure temperature is monitored by an MCP9808 temperature sensor. The heating element is kept in this enclosure to maintain the temperature isolated from room temperature. The temperature sensor has Inter-Integrated Circuit (I2C) communications capabilities and communicates with the mbed ARM microcontroller. The microcontroller compares the set point to the temperature of the heated enclosure. The result comparison of the reference point to the current temperature of the system is called the error signal. Afterwards, the error signal can be used as control point in a close-loop system.

The system increases voltage if the current temperature is too low, likewise, if the existing temperature is too high for the system, the system reduces the voltage output. How the system increases and decreases the system voltage exclusively depends on the feedback loop strategy being implemented. A simplified close-loop system diagram for this project is illustrated in Fig 7.

The mbed LPC1768 board provides a digital pulse-width modulation that could be set to significantly high frequencies that can efficiently drive the BC. The mbed board also provides a 32-bit ARM 96MHz Cortex that could be utilized for all the calculations required by the controller, filtering and linearization function k_e. In addition, an external circuit was built to drive the MOSFET at both the desired voltage and frequency. An example of how the duty cycle of the pulse-width modulation occurs can be seen in Fig 8.

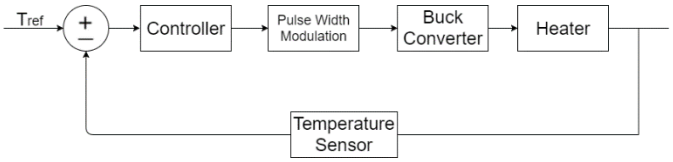

Fig. 7. Basic diagram of a closed-loop system.

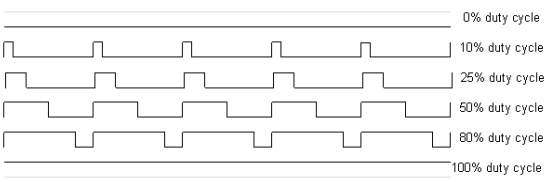

Fig. 8. Duty cycle percentages [9].

The MOSFET driver circuit has an operating voltage of 12V and requires a 5V PWM signal. The mbed microcontroller operates at 3.3V. However, the driver circuitry requires a PWM input of 5V. This was solved by including a Low-Power Dual-Channel Digital Isolator. The isolator takes the 3.3V PWM input and outputs a 5V PWM with the same frequency and duty cycle. The isolator also isolates the microcontroller from the analog side of the circuit with a semiconductor isolation barrier. A 12V voltage regulator was added to regulate the voltage and output of the MOSFET driver. Also, a 5V voltage regulator is used to regulate the output of the Dual-Channel Digital Isolator.

Other miscellaneous items used in the circuit design include: terminal connectors for I2C connection and the 12V PWM driver IC, barrel connector for the power supply and a right-angle switch to turn on/off the power applied to the circuit. The schematic and the board layout can be seen in Fig 9 and Fig 10.

Digital multimeters with data logging capability were chosen to measure the power inputs to the both Bang-Bang and BC systems. Agilent 34410A digital multimeters were utilized for this purpose to measure both DC/AC voltages and currents. The voltage and current values were logged to a local laptop PC through a RS232 serial connection.

The procedure to measure both Bang-Bang controller and Buck converter voltages/currents is shown in Fig. 11.

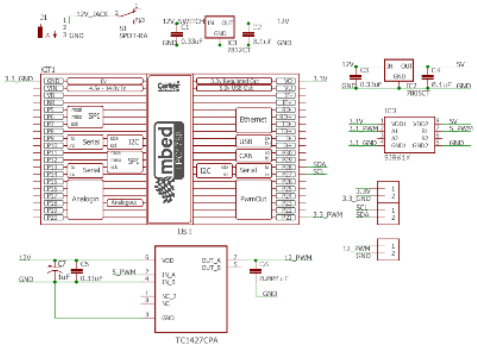

Fig. 9. Schematic layout of PWM MOSFET driver.

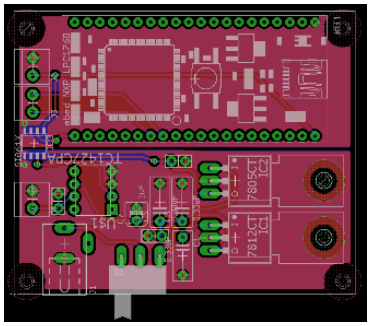

Fig. 10. Board layout of PWM MOSFET driver.

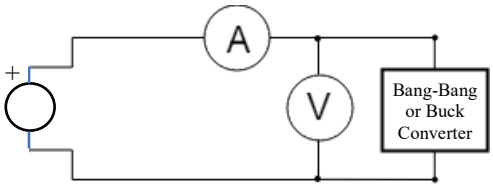

Fig. 11. Power measurement scheme for bang-bang or buck converter

To utilize the serial communication feature from the digital multimeters, a few accommodations were made, considering that most modern computers do not have built in serial interface. A 9-pin null male to male connector is attached to the multimeter, followed by a Universal Serial Bus (USB) Serial connector to the computer. The physical setup can be seen in Fig 6. To enable serial communication on an Agilent multimeter, 'Talk Only' mode must be enabled and set. This is achieved by setting GPIB address to '31' in the front-panel I/O Menu of the multimeter. Subsequently, the RS232 communication protocol must be configured and set. The I/O menu can set the baud rate, data bits, parity and stop bits.

On the computer side, serial communication is usually configured and connected through software. When the RS232 USB interface connector is used, it is important to confirm the correct communication (COM) port is utilized by the computer to communicate to the multimeters. It is also essential that the software being utilized supports logging of data; most modern serial communication tools support this feature. An example of a computer software serial configuration in software is shown in Fig 12.

V. Results

The results investigate the different solutions that were obtained through the implementation of proposed methods. The first section analyzes the linearization of the system. The second section compares the performance of the controller with BC and the traditional Bang-Bang controller. Two main factors that are examined of temperature disparity and more importantly energy consumption. The third section focuses on modeling the temperature system utilizing second order modeling functions. And finally, the results explore the validation of the thermal models developed via simulations in MATLAB/Simulink environment.

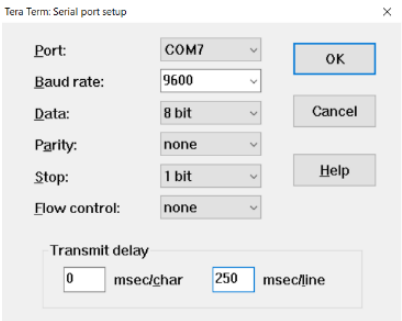

Fig. 12. Software serial COM configuration

A. *Linearization*

The main focus of this research is the linearization of the thermal power generation. The input of the buck converter d_R must have linearly related to the output power P of the buck converter. Fig. 13 displays how the voltage (in blue) reacts to d_R input of the system. It is clear that the voltage to d_R ratio is not constant and linearity is questionable. However, the power response to d_R ratio is approximately constant as expected or linear after 900 s. Due to the limitations in BC's output voltage (or 100% limit in duty cycle), early part of Fig. 13 before 900 s is variable for both cases and linearity cannot be justified. This is primarily because of the fact that the voltage output of the BC cannot keep up with the proportional controller's output and hits the upper saturation limit.

B. *Comparison to traditional heating method*

Bang-Bang controller is the traditional heating method application. A Bang-Bang controller processes the error when the current temperature is compared to the set point temperature which is selected by the user. A Bang-Bang controller has two states ON or OFF. It is a basic feedback system, if the current temperature is less than the set point plus or minus the tolerance the system will be ON. Otherwise, the system meets the desired temperature range and the system will be in the OFF state. Because of the natural temperature dissipation, the temperature falls and cools the system, eventually the temperature would continue to decrease until the Bang-Bang controller needs to change to the ON state. The time and temperature that the system utilizes to warm up and cool down is called the system cycle. The Bang-Bang controller is often used because of the simplicity of the control mechanism.

To compare the Bang-Bang controller and the P-Only controller utilizing the buck converter fairly the Bang-Bang controller was set to an initial temperature. Unfortunately, because of the nature of the Bang-Bang controller and the built-in tolerance of the controller when utilizing this controller, the temperature achieved is not really equal to the set temperature. To deal with this inconsistency, an average temperature of the heated space was calculated through the whole heating and cooling cycle.

After the averaging procedure, the temperature set point for the buck converter heating application was decided. It is important to note that proportional controller cannot also achieve perfect tracking for reference temperature. Therefore, a trial and error process for proper reference temperature selection was applied. This process aims the equality of temperature integrals for the duration of the test.

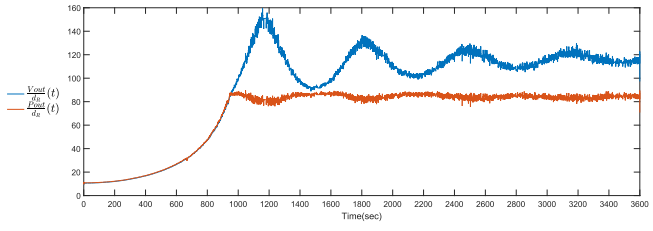

Fig. 13. BC voltage V_{out} to d_R ratio (blue) and power to d_R ratio (red)

The comparison of the Bang-Bang controller and the BC temperature profiles for 1 hour duration can be seen in Fig 14. The results demonstrated that the temperate profile is approximately constant for the BC at steady state with less temperature disparity.

The power drawn for both systems was measured utilizing the Agilent 34410A as discussed earlier. The placement of measurement devices for both controllers has critical importance for a fair judgement. The digital multimeters for the Bang-Bang controller (Love Series 16A) is set directly before the semiconductor triac switch and measured rms current and voltage values. Meanwhile, the digital multimeters for the buck converter's input power measurement were placed right after 86V DC source in reference to Fig. 5 and Fig. 11. In this case, the meters were configured for DC current and voltage measurement. Logged voltage and current values were eventually multiplied to calculate active/average power drawn. A sample power input profiles for both cases can be seen in Fig. 15.

C. *Thermal Modeling*

The thermal system was identified through the second order mathematical model used in the prior research [2]. Identified thermal circuit equivalent for this model can be seen in Fig. 16. R_1 cannot be identified due to the construction of the model. The model input/output variables include electrical power input P_{in}, heated space temperature output T_{room}, and ambient temperature input $T_{ambient}$. The identified system parameters are used to calculate temperature output T_{room} based on given temperature input $T_{ambient}$ and electrical power input P_{in}.

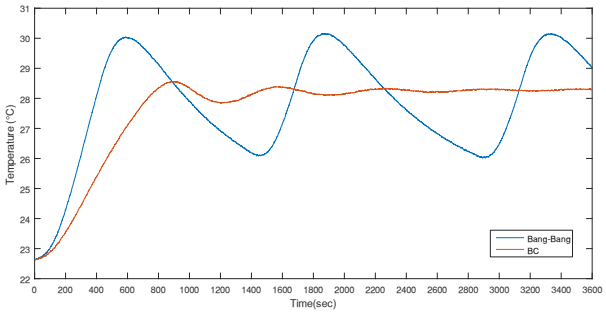

Fig. 14. Temperature profiles with bang-bang and buck converter

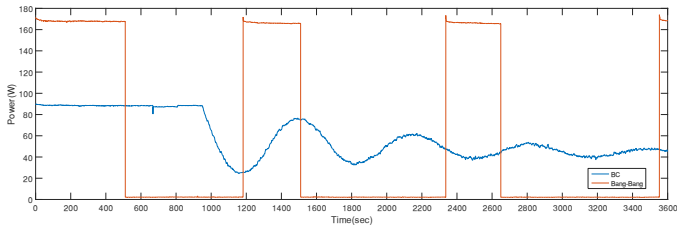

Fig. 15. Power profiles with bang-bang and buck converter

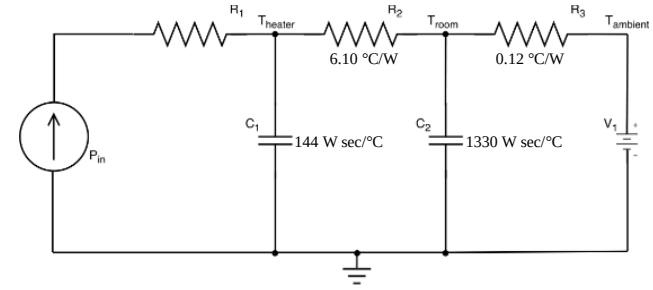

Fig. 16. Identified thermal circuit model

Fig 17 displays how the physical system response and the model compares. Quality of fit between these two waveforms is 93.2% as shown in Fig. 17. According to the figure, the simulated and the actual system transients closely match while the responses towards steady state also compare reasonably well.

D. *Model Validation*

Utilizing the identified thermal circuit model, a feedback loop controller model was designed utilizing Simulink, and can be seen in Fig 18. The model duplicates all parts of the experimental controller system. The first block from left is the controller, which accounts for the linearization function of the system. A breakdown of the controller subsystem titled "P-Controller" can be seen in Fig 19. Since the proportional controller is only multiplying by one, the proportion was left out of the current subsystem.

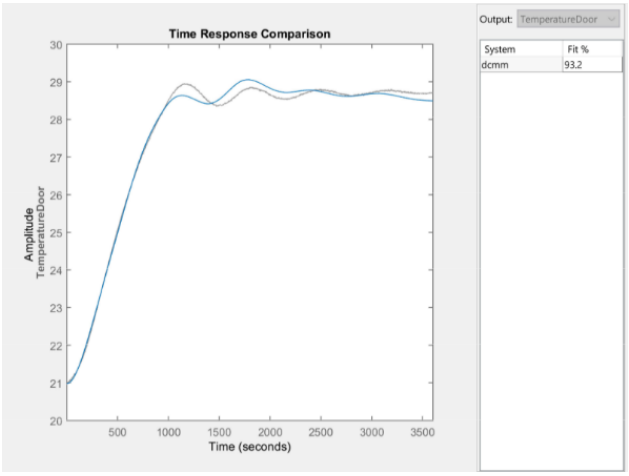

Fig.17. Modelled (blue) vs actual heated space temperatures (gray)

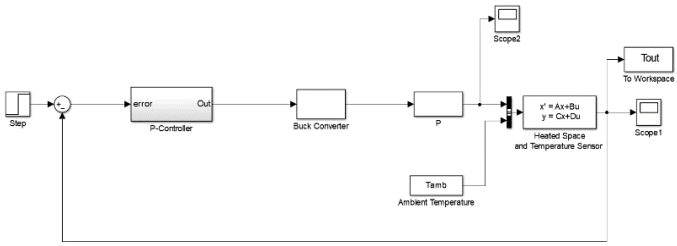

Fig. 18. Simulink block diagram

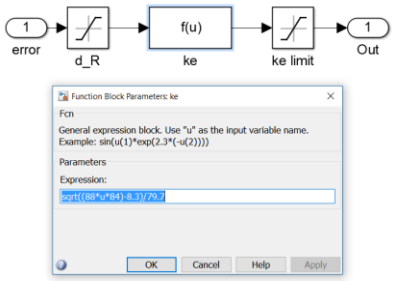

Fig. 19. P-Controller with linearization function

The first saturation block (d_R) in the subsystem limits the input to positive values for the linearization block k_e to account for the square root function. After the linearization block, the k_e saturation block is used. This block models the real constraints of the BC. The output is limited from 5 to 100 percent of the duty cycle as explained in Section III. B.

The next blocks in the model simulate the linear gain of the BC as well as the final output power conversion of the system. The inputs of the thermal model identified earlier includes the electrical power by the BC as well as the ambient temperature. A final simulated output of the system is the temperature for the heated space and is shown in Fig. 20. Along with the simulated temperature Fig. 20 also plots the real temperature response of the system for the same inputs, displaying the similarities between real and simulated temperature. Earlier part of the transient state of the simulated system fits the real data almost perfectly. The later part of transient state response has some minor difference. Steady state response also matches each other very closely. This simulation is later used to determine how the system reacts to different controller algorithms and techniques. A real test takes about an hour to complete, with the model developed it will be known how the system approximately reacts almost instantaneously. The model can run a simulated test multiple times to ensure that the results are evaluated before a real test is attempted.

VI. CONCLUSION

A linear thermal power controller was designed and implemented by involving various technical aspects such as power electronics, digital signal processing, and linear control theory. The buck converter with a linearization mechanism was successfully tested and validated for expected behavior through experiments. In addition, the new heater control framework reduced temperature disparity significantly. A second order thermal model utilizing an equivalent circuit was also identified and validated using Simulink simulations and physical experiments.

Future work will include a developed data collection method for energy consumption and comparison between two controllers. Due to the linearity of control shown in this work, the other feedback control methods such as proportional integral controller and/or other optimal control methods can be investigated for efficiency improvement in the future.

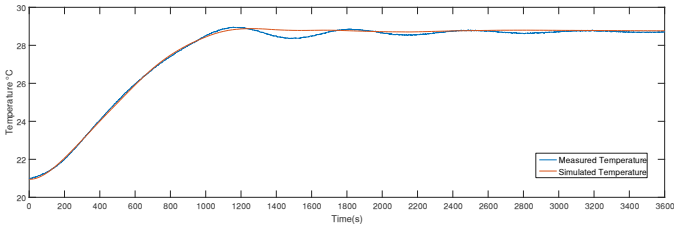

Fig. 20. Simulated vs measured temperature

Furthermore, higher order linear filtering methods such as Butterworth or Chebyshev filters will be tested for performance improvement in comparison to the IIR filter.

ACKNOWLEDGMENT

The authors wish to thank the Graduate School and Research at Western Carolina University for supporting this project.

REFERENCES

[1] "Energy Use in Homes - Energy Explained, Your Guide To Understanding Energy - Energy Information Administration", *eia.gov*, 2017. [Online]. Available: https://www.eia.gov/energyexplained/index.cfm/data/index.cfm?page=us_energy_homes. [Accessed: 10- Apr- 2017].

[2] H. Karayaka, L. Holland, M. Tanaka and A. Ball, "Power Systems: Thermal Load Characterization and Regulation", *Encyclopedia of Energy Engineering and Technology, Second Edition*, pp. 1-23, 2014.

[3] D. Hammerstrom, N. Lu and J. Kondoh, "An evaluation of the water heater load potential for providing regulation service", *IEEE Transactions on Power Systems*, vol. 26, no. 3, pp. 1309-1316, 2011.

[4] L. Holland, H. Karayaka, M. Tanaka and A. Ball, "An Investigation of Parametric Load Leveling Control Methodologies for Resistive Heaters in Smart Grids", *2014 Sixth Annual IEEE Green Technologies Conference*, 2014.

[5] L. Holland, H. Bora Karayaka, M. Tanaka and A. Ball, "An empirical method for estimating thermal system parameters based on operating data in smart grids", *ISGT 2014*, 2014.

[6] S. Gupta, *Elements of control systems*, 1st ed. Upper Saddle River, N.J.: Prentice Hall, 2002.

[7] N. Macia and G. Thaler, *Modeling and control of dynamic systems*, 1st ed. Clifton Park: Thomson Learning, 2005.

[8] H. Bischoff and D. Hofmann, *Process Control System*, 1st ed. Dresden: Festo Didactic GmbH & Co., 1997.

[9] "Arduino - SecretsOfArduinoPWM", *Arduino.cc*, 2017. [Online]. Available: https://www.arduino.cc/en/Tutorial/SecretsOfArduinoPWM. [Accessed: 24- Apr- 2017].

[10] "Arduino - Compare", *Arduino.cc*, 2017. [Online]. Available: https://www.arduino.cc/en/Products/Compare. [Accessed: 21- Apr- 2017].

[11] M. Vanouni and N. Lu, "Improving the Centralized Control of Thermostatically Controlled Appliances by Obtaining the Right Information", *IEEE Transactions on Smart Grid*, vol. 6, no. 2, pp. 946-948, 2015.

[12] *Control Systems Theory With Engineering Applications*, 1st ed. Birkhauser, 2013.

[13] O'Dwyer, *Handbook of PI and PID controller tuning rules*, 3rd ed. London: Imperial College Press, 2009.